Chapter 5

Numerical results: Isotropic plates and shells

In this chapter numerical results are presented for the isotropic plate and shell elements presented in Chapter 4.

In the following,

- SA denotes the Bathe-Dvorkin assumed strain plate element [7].
- QI denotes the incompatible modes element presented by Ibrahimbegovic [54].
- QC9D/SA and QC9D*/SA denotes the flat shell elements that are formed by combining the QC9D membrane element of Ibrahimbegovic *et al.* and the Bathe-Dvorkin assumed strain plate element, respectively with and without the locking correction.
- 5β/SA denotes the flat shell element that is formed by combining the 5β-NT membrane element and the Bathe-Dvorkin assumed strain plate element.
- 8β-NC/SA, 8β-NT/SA, $8\beta*$-NC/SA and $8\beta*$-NT/SA denotes the flat shell elements that are formed by the 8β(D) membrane element combined with the Bathe-Dvorkin assumed strain plate element, respectively with and without the locking correction.
- 9β-NC/SA, 9β-NT/SA, $9\beta*$-NC/SA and $9\beta*$-NT/SA denotes the flat shell elements that are formed by the 9β(D) membrane element combined with the Bathe-Dvorkin assumed strain plate element, with and without the locking correction.

The notation '(incl. RBF)' indicates that the following residual bending flexibility correction,

$$\begin{aligned} \frac{1}{G*} &= \frac{1}{G} + \frac{l^2}{Eh^2} \\ &= \frac{1}{G}\left(1 + \frac{l^2}{2(1+\nu)h^2}\right) \end{aligned} \tag{5.1}$$

is included [13, 45, 55], where the term l^2/Eh^2 is denoted the residual bending flexibility in [55].

A shear rigid formulation is obtained by setting the shear correction factor $k \to \infty$ [52].

5.1 Plate patch tests

The plate elements used in this study passed the following patch tests:

- Constant curvature patch test (See Figure 5.1)
- Constant shear patch test with zero rotations (See Figure 5.1)
- Constant twist patch test (See Figure 5.2)

However, the constant twist patch test depicted in Figure 5.2 is passed exactly for thin plates only. Since the plate is exactly the same as the original formulation of Bathe and Dvorkin, these results are not repeated here. (See [7, 47]).

The residual bending flexibility correction is not included in the patch tests. However, the element rank stays unchanged as a result of the residual bending flexibility correction.

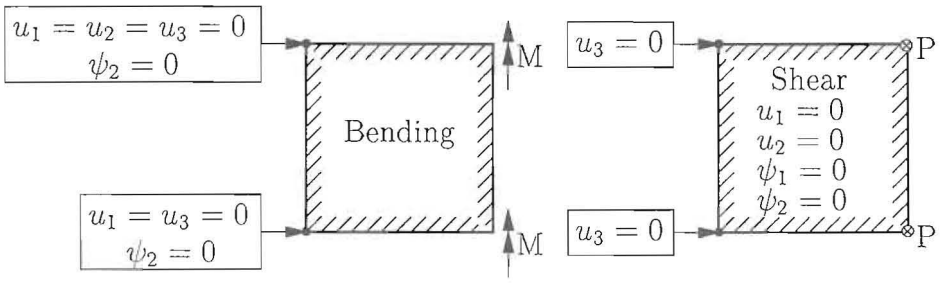

Figure 5.1: Constant curvature patch test and constant shear patch test with zero rotations

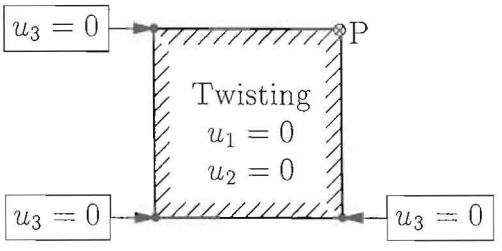

Figure 5.2: Constant twist patch test

5.2 Cantilever under transverse tip loading

This simple one-dimensional problem is taken from Bathe and Dvorkin [47]. The geometry and the material properties are depicted in Figure 5.3. Normal 4-node elements employing bi-linear bending shape functions can only represent this problem in the limit of mesh refinement, since the elements only have a constant strain capability. Table 5.1 reveals that the residual bending flexibility correction raises the capability of the 4-node element to the linear strain level for this problem.

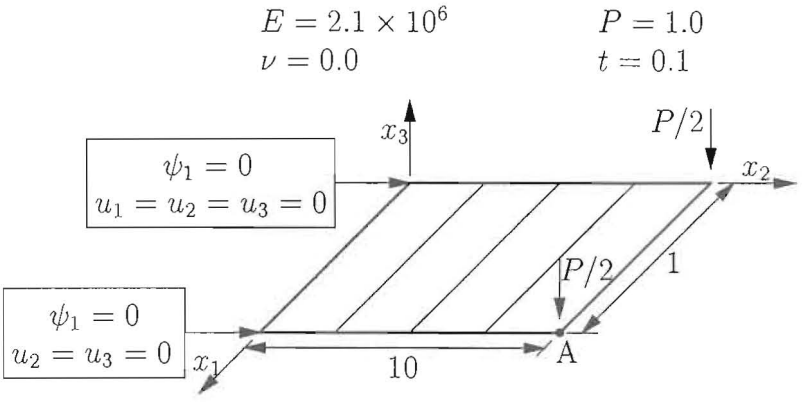

Figure 5.3: Cantilever under transverse tip loading

5.3 Thin simply supported plate under uniformly distributed load

This problem (See Figure 5.4) is included to illustrate the effect of the residual bending flexibility correction on thin plates [54]. Moreover, the effect of the degree of support at the boundaries ($x_1 = l/2$, $x_1 = -l/2$, $x_2 = l/2$ and $x_2 = -l/2$) is also illustrated. Two conditions are considered, namely hard support and soft support. For the soft supported condition the theoretical solution is unknown. The central deflection, $-u_{3_A}$, is measured.

Tables 5.2 and 5.3 show that the QI and SA(incl. RBF) elements converge from above, while the SA and SA($k \to \infty$) elements converge form below.

For both support conditions the results obtained with the SA element are superior to the results obtained with both QI and SA(incl. RBF).

5.4 Pinched hemispherical shell with 18^o hole

This problem forms part of the set proposed by MacNeal and Harder [45]. This doubly-curved shell problem is characterized by inextensible bending modes and large rigid body rotations [56]. The geometry is depicted in Figure 5.5, and tabulated numerical results are

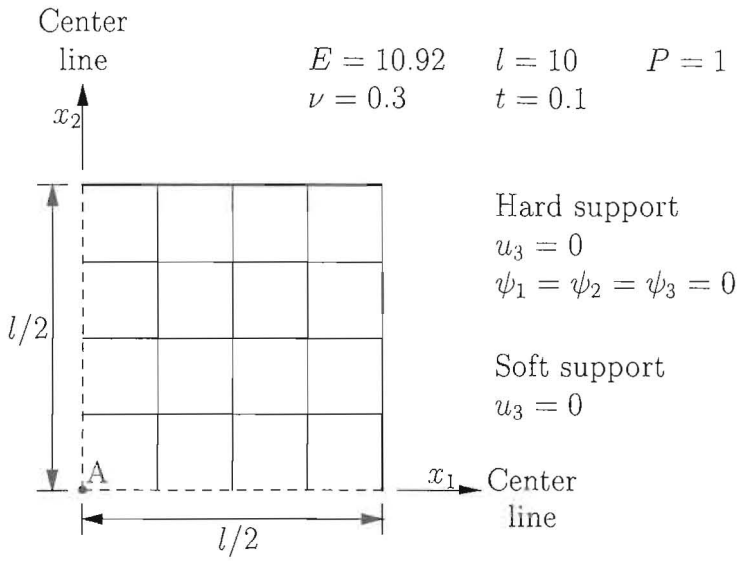

Figure 5.4: Thin simply supported plate under uniformly distributed load

presented in Table 5.4. The exact solution is 0.094 [45], although more recent analyses suggest 0.093 [20].

The results obtained with the 8β/SA and 9β/SA families are almost identical. 5β/SA outperform the 8β/SA and 9β/SA families for a coarse mesh. Note that the NC-formulations are more accurate than the NT-formulations for the coarse mesh.

The influence of γ on this problem is very small, although for small values of γ the accuracy improves slightly. The results are reflected in Table 5.5. The choice of $\gamma = G$ results in good accuracy.

For the coarse mesh the elements with the membrane locking correction using the 8-point integration scheme outperforms the other combinations of integration schemes with and without the locking correction (see Table 5.6).

5.5 Warped pinched hemisphere

In Figure 5.6 the geometry and the discretization of the warped pinched hemisphere is depicted. The chosen discretization implies that quadrilateral flat shell elements become highly warped. Mesh refinement is obtained by bisection. Note that the warpage does not disappear in the limit of mesh refinement.

The exact analytical solution was presented by Parisch [56], which compares well with the solution of the pinched hemisphere with 18° hole, since additional elements in the top of the hemisphere are expected to contribute only slightly towards the overall stiffness of the shell under pinching loads. This problem is also dominated by inextensible bending modes and large rigid body rotations [56].

Table 5.7 reveals that the 5β/SA element outperforms all the other elements for this test. Very little detrimental effect due to the out-of-plane warp is evident. Still, the warp correc-

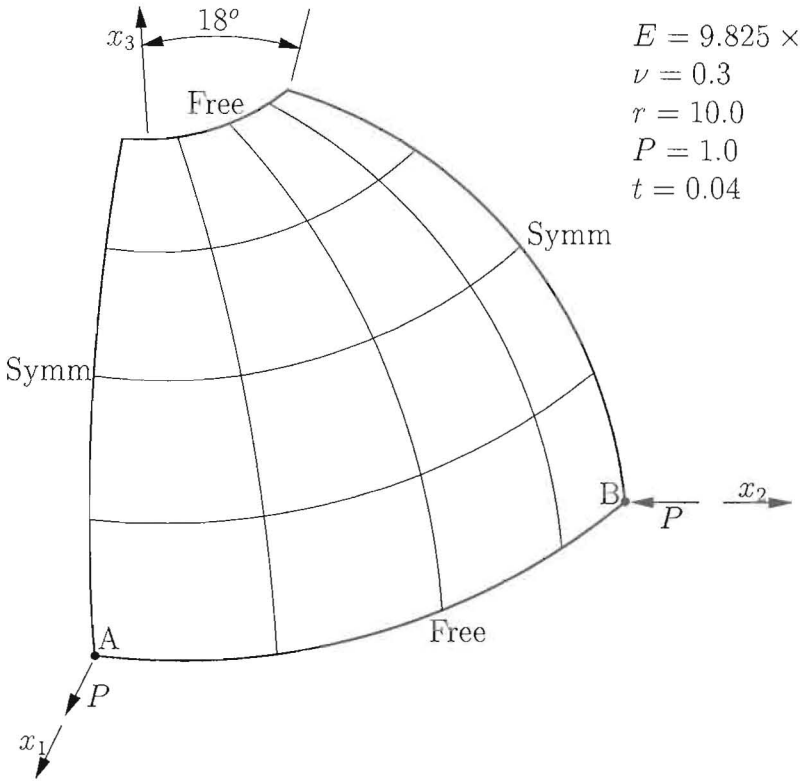

Figure 5.5: Pinched hemisphere

tion, (4.65), is crucial.

5.6 Thick pinched cylinder with open ends

The pinched cylinder problem is dominated by inextensible bending behavior and results will reveal any tendency towards membrane-bending locking [6]. In Figure 5.7 the geometry and the discretization are depicted.

Table 5.8 reveals that the NC-formulations are the most accurate for the coarse mesh. In general, the locking correction improves the element behavior for this problem.

5.7 Thin pinched cylinder with open ends

This problem is identical to the previous, except for a thiner wall thickness (Figure 5.7). Table 5.9 illustrates that all the elements tested perform almost identically, since the drilling degrees of freedom are not activated due to the pinching loads. The locking correction only slightly improves the performance of the elements.

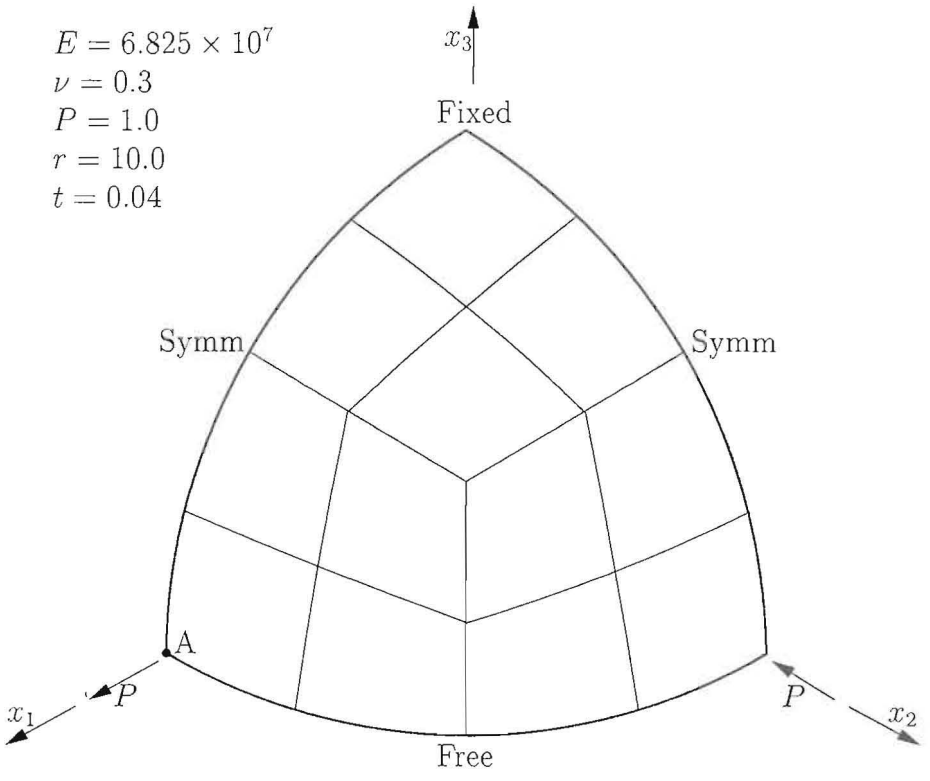

Figure 5.6: Warped pinched hemisphere

5.8 Pinched cylinder with end membranes

This problem is also dominated by inextensible bending behavior (See Figure 5.8). However, this problem is regarded as more difficult than the pinched cylinder with open ends [47].

From Table 5.10 it can be seen that that all the elements tested perform almost identically. (Once again, the drilling degrees of freedom are not activated due to the pinching loads.)

5.9 Thick pre-twisted beam

This problem is in the set proposed by MacNeal and Harder [45]. Results are presented by Taylor[6]. The thick pre-twisted beam depicted in Figure 5.9 is used to illustrate the capability of the elements for warped geometries.

Numerical results for this problem are tabulated in Table 5.11. All the elements tested perform almost identically for this test. The 5β/SA element is not included in this test, because the lack of drilling degrees of freedom complicates the use of this element for this geometry. This shows that the drilling degrees of freedom are a necessity for the problem.

$r = 4.953$
$l = 10.35$
$E = 10.5 \times 10^6$
$\nu = 0.3125$

Thick $\begin{cases} t = 0.094 \\ P = 100.0 \end{cases}$

Thin $\begin{cases} t = 0.01548 \\ P = 0.1 \end{cases}$

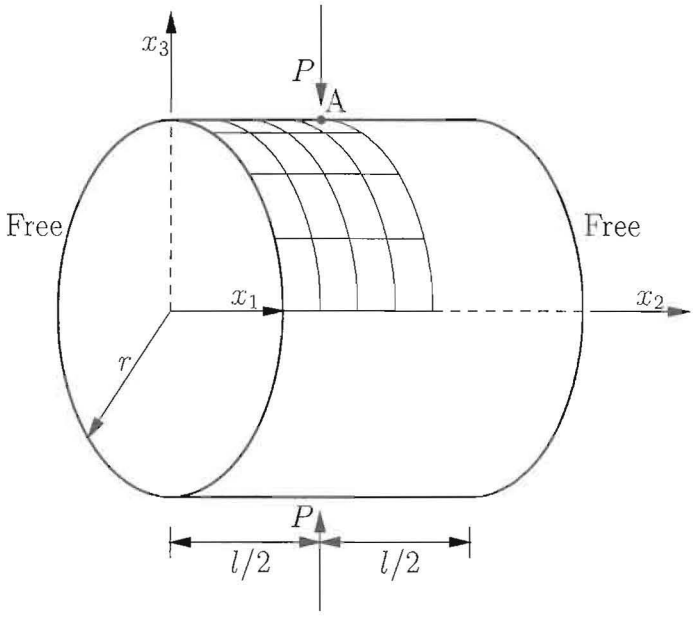

Figure 5.7: Pinched cylinder with open ends

5.10 Thin pre-twisted beam

Jetteur [16] proposed this problem, and this problem is used to evaluate locking. Results are presented by Taylor[6]. The thin pre-twisted beam is also depicted in Figure 5.9.

Numerical results for this problem are tabulated in Table 5.12. Again, all the elements perform virtually identical and are very accurate.

5.11 Scordelis-Lo roof

In Figure 5.10 the geometry and the discretization of this problem is depicted. The analytical solution of the mid-side vertical displacement, u_{3_A}, is normally taken as 0.3024 [45], even though a value of 0.3086 was originally presented by Scordelis and Lo [57].

The NT-formulations and the QC9D element outperform the other elements (Table 5.13).

5.12 Slender cantilever

MacNeal and Harder [45] proposed this problem to illustrate the effect of mesh distortion and element aspect ratio (See Figure 5.11, Table 5.14). Three shapes are considered, namely

$E = 3.0 \times 10^6$ $\quad r = 300.0$
$\nu = 0.3$ $\quad l = 600.0$
$P = 1.0$ $\quad t = 3.0$

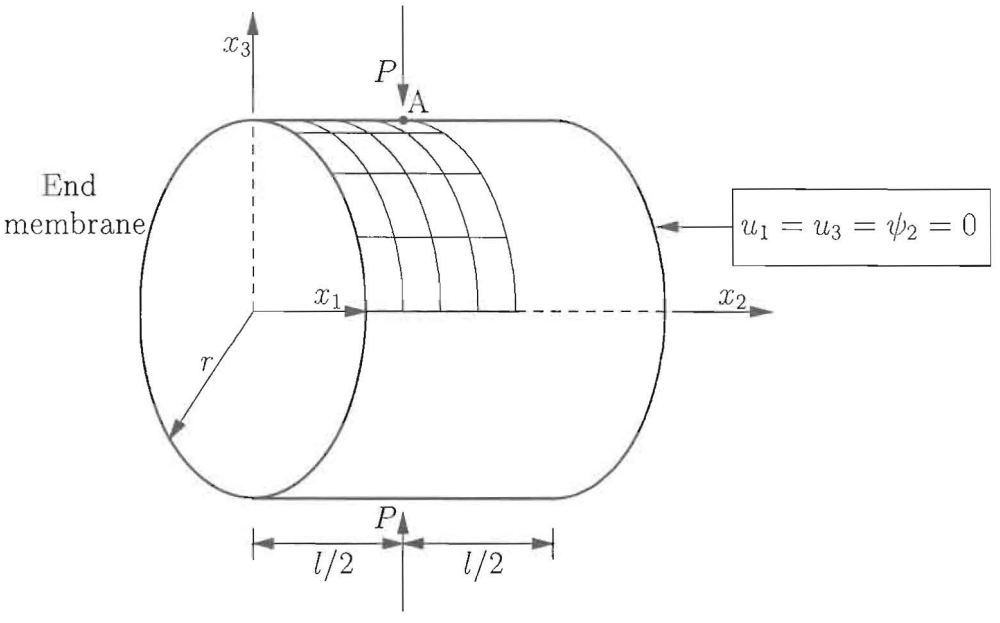

Figure 5.8: Pinched cylinder with end membranes

- regular shaped elements, $\alpha_i = 0^o$ for $i = 1, 2, 3, 4, 5$,
- parallelogram shaped elements, $\alpha_i = 45^o$ for $i = 1, 2, 3, 4, 5$, and
- trapezoidal shaped elements, $\alpha_i = 135^o$ and $\alpha_j = 45^o$ for $i = 1, 3, 5$ and $j = 2, 4$.

The clamped boundary condition prescribed by MacNeal and Harder for the beam does not allow modeling of the pure extensional force field for non-zero values for Poisson's ratio ($\nu \neq 0$) with membrane elements. For this reason the extension test was modified so that only the required restraints, two in the longitudinal and one in the thickness direction, are modeled [52].

For all the meshes all the elements converge to the exact answer for the unit extensional load case, except the NC-formulation without the locking correction for the regular mesh. For the out-of-plane shear and the twisting forces all the elements yields identical results for all the meshes. Even for the irregular meshes the elements perform very well.

For the in-plane shear test the 5β/SA element is the most accurate, while the NT-formulation are also very accurate for the regular mesh. For the irregular meshes the 5β/SA element is not accurate, while the $8\beta*$-NT/SA element still gives accurate results.

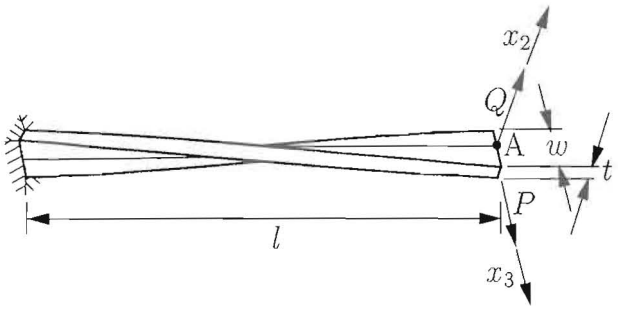

$E_{11}/E_{22} = 40$ $\quad w = 1.1$
$E_{22}/G_{23} = 2$ $\quad l = 12$
$E_{22}/G_{13} = 5/3$ $\quad$ Thick: $t = 0.32$
$E_{22}/G_{12} = 5/3$ $\quad$ Thin: $t = 0.05$
$\nu_{12} = 0.28$ $\quad P = 1$
$Q = 1$

Figure 5.9: Pre-twisted beam

$E = 432 \times 10^6$ $\quad l = 50.00$
$\nu = 0.0$ $\quad r = 25.0$
Load =90/unit shell area (weight) $\quad t = 0.25$

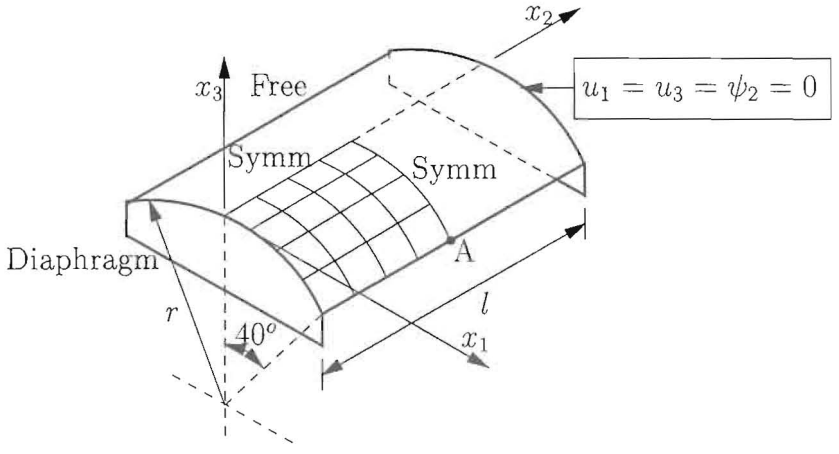

Figure 5.10: Scordelis-Lo roof

Element	1×1	1×4
SA	1.429	1.875
SA(incl. RBF)	1.905	1.905
Exact solution	1.905	

Table 5.1: Cantilever under transverse tip loading: Tip displacement u_{3_A}

$E = 1.0 \times 10^7$ $P = 1$ $t = 0.1$
$\nu = 0.30$ $l = 6.0$ $h = 0.2$

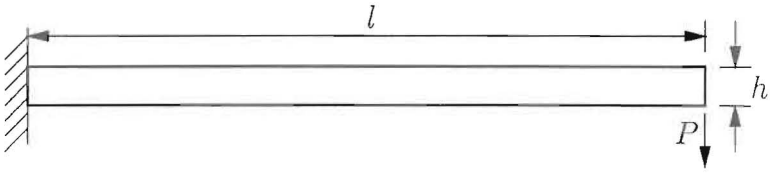

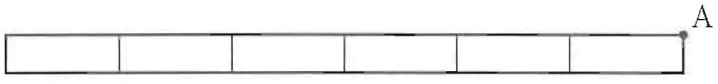

Regular mesh

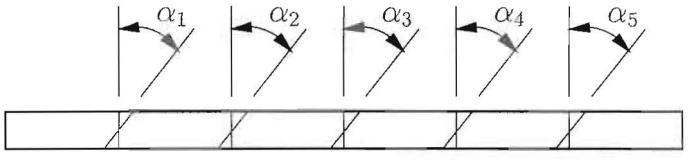

Irregular mesh

Figure 5.11: Slender cantilever

Element	2×2	4×4	8×8	16×16	32×32
SA	39712	40436	40593	40632	40641
SA($k \to \infty$)	39690	40414	40572	40612	40625
SA(incl. RBF)	44141	41499	40854	40694	40654
QI [54]	42512	41115	40761	40673	40651
Plate theory [58]			40644		

Table 5.2: Thin simply supported plate under uniformly distributed load (Hard supported): Center displacement $-u_{3_A}$

Element	2×2	4×4	8×8	16×16	32×32
SA	39728	40466	40653	40747	40841
SA($k \to \infty$)	39690	40414	40572	40612	40625
SA(incl. RBF)	46550	42774	41533	41089	40948
QI [54]	44613	42273	41395	41060	40961

Table 5.3: Thin simply supported plate under uniformly distributed load (Soft supported): Center displacement $-u_{3_A}$

Element	2×2	4×4	8×8	16×16	32×32
5β/SA	0.08420	0.09330	0.09292	0.09313	0.09346
QC9D/SA	0.006745	0.01135	0.05953	0.08987	0.09318
8β-NC/SA	0.01202	0.05681	0.08483	0.09278	0.09348
8β-NT/SA	0.007731	0.01304	0.06408	0.09053	0.09322
9β-NC/SA	0.01185	0.05606	0.08459	0.09276	0.09348
9β-NT/SA	0.006939	0.01226	0.06145	0.09015	0.09320
QC9D$*$-SA	0.006554	0.01047	0.05905	0.08998	0.09324
$8\beta*$-NC/SA	0.009182	0.03363	0.08394	0.09297	0.09355
$8\beta*$-NT/SA	0.007268	0.01177	0.06329	0.09063	0.09328
$9\beta*$-NC/SA	0.008982	0.03334	0.08372	0.09295	0.09355
$9\beta*$-NT/SA	0.006809	0.01116	0.06087	0.09026	0.09326
Best known [20]			0.09300		

Table 5.4: Pinched Hemisphere with 18^o Hole: Radial displacement u_{1_A}

γ	2×2
$G \times 10^{-3}$	0.008067
$G \times 10^{-2}$	0.008057
$G \times 10^{-1}$	0.007975
$G \times 10^{0}$	0.007731
$G \times 10^{1}$	0.007605
$G \times 10^{2}$	0.007586
$G \times 10^{3}$	0.007584
Best known	0.093000

Table 5.5: Pinched Hemisphere with 18^o Hole: Influence of γ for the 2×2 mesh

Element	2×2	4×4	8×8	16×16
5 point integration				
$8\beta*$-NC/SA	0.01087	0.05721	0.09174	0.09362
$8\beta*$-EP/SA	0.008424	0.03635	0.08937	0.09312
$8\beta*$-OC/SA	0.007254	0.03604	0.08939	0.09312
$8\beta*$-NT/SA	0.007338	0.03612	0.08939	0.09312
$8\beta*$-PH/SA	0.007274	0.03492	0.08926	0.09311
8β-NC/SA	0.02543	0.08607	0.09311	0.09343
8β-EP/SA	0.02981	0.08757	0.09270	0.09307
8β-OC/SA	0.02600	0.08707	0.09272	0.09308
8β-NT/SA	0.02603	0.08707	0.09272	0.09308
8β-PH/SA	0.01494	0.08287	0.09262	0.09307
8 point integration				
$8\beta*$-NC/SA	0.01088	0.05733	0.09175	0.09362
$8\beta*$-EP/SA	0.008416	0.03601	0.08922	0.09311
$8\beta*$-OC/SA	0.007309	0.03598	0.08926	0.09311
$8\beta*$-NT/SA	0.007430	0.03607	0.08926	0.09311
$8\beta*$-PH/SA	0.007276	0.03457	0.08909	0.09310
8β-NC/SA	0.02530	0.08596	0.09312	0.09344
8β-EP/SA	0.02452	0.08532	0.09253	0.09306
8β-OC/SA	0.03495	0.08610	0.09257	0.09307
8β-NT/SA	0.03507	0.08612	0.09257	0.09307
8β-PH/SA	0.01425	0.08045	0.09243	0.09306
Full integration				
$8\beta*$-NC/SA	0.009182	0.03363	0.08394	0.09297
$8\beta*$-EP/SA	0.007056	0.01176	0.06330	0.09063
$8\beta*$-OC/SA	0.007299	0.01182	0.06333	0.09063
$8\beta*$-NT/SA	0.007268	0.01177	0.06329	0.09063
$8\beta*$-PH/SA	0.006586	0.01120	0.06141	0.09035
8β-NC/SA	0.01202	0.05681	0.08483	0.09278
8β-EP/SA	0.007667	0.01306	0.06409	0.09053
8β-OC/SA	0.008486	0.01311	0.06411	0.09053
8β-NT/SA	0.007731	0.01304	0.06408	0.09053
8β-PH/SA	0.006829	0.01239	0.06208	0.09025
Best known		0.093		

Table 5.6: Pinched Hemisphere with 18° Hole: Effect of integration scheme order

Element	2×2	4×4	8×8	16×16
5β/SA	0.08549	0.09086	0.09154	0.09185
QC9D/SA	0.0005911	0.006161	0.04522	0.08607
8β-NC/SA	0.001446	0.02180	0.07363	0.09068
8β-NT/SA	0.0006833	0.007153	0.04885	0.08692
9β-NC/SA	0.001439	0.02153	0.07339	0.09066
9β-NT/SA	0.0006833	0.006864	0.04805	0.08674
QC9D$*$/SA	0.0004999	0.005915	0.04471	0.08614
$8\beta*$-NC/SA	0.001410	0.01910	0.07212	0.09085
$8\beta*$-NT/SA	0.0005637	0.006761	0.04813	0.08697
$9\beta*$-NC/SA	0.001402	0.01890	0.07190	0.09083
$9\beta*$-NT/SA	0.0005637	0.006519	0.04736	0.08680
Analytical [56]		0.09240		

Table 5.7: Warped pinched hemisphere: Radial displacement u_{1_A}

Element	2×2	4×4	8×8	16×16
5β/SA	0.07026	0.1002	0.1100	0.1128
QC9D/SA	0.07005	0.09980	0.1099	0.1128
8β-NC/SA	0.07088	0.1005	0.1101	0.1129
8β-NT/SA	0.07008	0.09990	0.1099	0.1128
9β-NC/SA	0.07088	0.1005	0.1101	0.1129
9β-NT/SA	0.07005	0.09982	0.1099	0.1128
QC9D$*$/SA	0.07001	0.09979	0.1099	0.1128
$8\beta*$-NC/SA	0.07019	0.1007	0.1102	0.1129
$8\beta*$-NT/SA	0.07002	0.09986	0.1099	0.1128
$9\beta*$-NC/SA	0.07019	0.1007	0.1102	0.1129
$9\beta*$-NT/SA	0.07001	0.09981	0.1099	0.1128
Jaamei [17]		0.094		

Table 5.8: Thick pinched cylinder with open ends: Radial displacement $-u_{3_A}$

Element	2×2	4×4	8×8	16×16
5β/SA	0.01562	0.02196	0.02383	0.02440
QC9D/SA	0.01561	0.02194	0.02380	0.02439
8β-NC/SA	0.01562	0.02200	0.02387	0.02442
8β-NT/SA	0.01561	0.02194	0.02381	0.02439
9β-NC/SA	0.01562	0.02200	0.02387	0.02442
9β-NT/SA	0.01561	0.02194	0.02380	0.02439
QC9D$*$/SA	0.01561	0.02194	0.02380	0.02440
$8\beta*$-NC/SA	0.01562	0.02197	0.02389	0.02443
$8\beta*$-NT/SA	0.01561	0.02194	0.02381	0.02440
$9\beta*$-NC/SA	0.01562	0.02197	0.02389	0.02443
$9\beta*$-NT/SA	0.01561	0.02194	0.02380	0.02440
Jaamei [17]		0.01548		

Table 5.9: Thin pinched cylinder with open ends: Radial displacement $-u_{3_A}$

Element	4×4	8×8	16×16
5β/SA	0.7175E-05	1.376E-05	1.792E-05
QC9D/SA	0.6824E-05	1.396E-05	1.787E-05
8β-NC/SA	0.8138E-05	1.412E-05	1.802E-05
8β-NT/SA	0.6888E-05	1.355E-05	1.787E-05
9β-NC/SA	0.8138E-05	1.412E-05	1.802E-05
9β-NT/SA	0.6831E-05	1.351E-05	1.787E-05
QC9D$*$/SA	0.6930E-05	1.350E-05	1.785E-05
$8\beta*$-NC/SA	0.8078E-05	1.411E-05	1.801E-05
$8\beta*$-NT/SA	0.6956E-05	1.354E-05	1.786E-05
$9\beta*$-NC/SA	0.8078E-05	1.411E-05	1.801E-05
$9\beta*$-NT/SA	0.6938E-05	1.352E-05	1.786E-05
Jaamei [17]		1.8248E-05	

Table 5.10: Pinched cylinder with end membranes: Radial displacement $-u_{3_A}$

Element	1×6	2×12	4×24	8×48
In-plane shear: u_{3_A}				
QC9D/SA	5.387E-03	5.405E-03	5.412E-03	5.416E-03
8β-NC/SA	5.387E-03	5.405E-03	5.412E-03	5.416E-03
8β-NT/SA	5.388E-03	5.405E-03	5.412E-03	5.416E-03
9β-NC/SA	5.387E-03	5.405E-03	5.412E-03	5.416E-03
9β-NT/SA	5.388E-03	5.405E-03	5.412E-03	5.416E-03
QC9D$*$/SA	5.387E-03	5.405E-03	5.412E-03	5.416E-03
$8\beta*$-NC/SA	5.387E-03	5.405E-03	5.412E-03	5.416E-03
$8\beta*$-NT/SA	5.388E-03	5.405E-03	5.412E-03	5.416E-03
$9\beta*$-NC/SA	5.387E-03	5.405E-03	5.412E-03	5.416E-03
$9\beta*$-NT/SA	5.388E-03	5.405E-03	5.412E-03	5.416E-03
Analytical [45]		5.429E-03		
Out-of-plane shear: u_{2_A}				
QC9D/SA	1.758E-03	1.755E-03	1.752E-03	1.753E-03
8β-NC/SA	1.757E-03	1.755E-03	1.752E-03	1.753E-03
8β-NT/SA	1.761E-03	1.756E-03	1.753E-03	1.753E-03
9β-NC/SA	1.757E-03	1.755E-03	1.752E-03	1.753E-03
9β-NT/SA	1.761E-03	1.756E-03	1.753E-03	1.753E-03
QC9D$*$/SA	1.758E-03	1.754E-03	1.752E-03	1.753E-03
$8\beta*$-NC/SA	1.757E-03	1.754E-03	1.752E-03	1.753E-03
$8\beta*$-NT/SA	1.761E-03	1.755E-03	1.753E-03	1.753E-03
$9\beta*$-NC/SA	1.757E-03	1.754E-03	1.752E-03	1.753E-03
$9\beta*$-NT/SA	1.761E-03	1.755E-03	1.753E-03	1.753E-03
Analytical [45]		1.750E-03		

Table 5.11: Thick pre-twisted beam: Numerical results

Element	1×6	2×12	4×24	8×48
In-plane shear: u_{3_A}				
QC9D/SA	1.383	1.384	1.386	1.387
8β-NC/SA	1.383	1.384	1.386	1.387
8β-NT/SA	1.383	1.384	1.386	1.387
9β-NC/SA	1.383	1.384	1.386	1.387
9β-NT/SA	1.383	1.384	1.386	1.387
QC9D*/SA	1.383	1.384	1.386	1.387
8β*-NC/SA	1.383	1.384	1.386	1.387
8β*-NT/SA	1.383	1.384	1.386	1.387
9β*-NC/SA	1.383	1.384	1.386	1.387
9β*-NT/SA	1.383	1.384	1.386	1.387
Isoparametric solid elements [16]			1.3857	
Out-of-plane shear: u_{2_A}				
QC9D/SA	0.3442	0.3434	0.3429	0.3429
8β-NC/SA	0.3442	0.3434	0.3429	0.3429
8β-NT/SA	0.3443	0.3434	0.3429	0.3429
9β-NC/SA	0.3442	0.3433	0.3429	0.3429
9β-NT/SA	0.3443	0.3434	0.3429	0.3429
QC9D*/SA	0.3442	0.3432	0.3429	0.3429
8β*-NC/SA	0.3442	0.3432	0.3429	0.3429
8β*-NT/SA	0.3443	0.3432	0.3429	0.3429
9β*-NC/SA	0.3442	0.3432	0.3429	0.3429
9β*-NT/SA	0.3443	0.3432	0.3429	0.3429
Isoparametric solid elements [16]			0.3427	

Table 5.12: Thin pre-twisted beam: Numerical results

Element	4×4	8×8	16×16
5β/SA	0.3162	0.3052	0.3074
QC9D/SA	0.3159	0.3038	0.3016
8β-NC/SA	0.3417	0.3107	0.3034
8β-NT/SA	0.3159	0.3038	0.3016
9β-NC/SA	0.3417	0.3107	0.3034
9β-NT/SA	0.3159	0.3038	0.3016
QC9D*/SA	0.3168	0.3041	0.3017
8β*-NC/SA	0.3428	0.3110	0.3034
8β*-NT/SA	0.3169	0.3041	0.3017
9β*-NC/SA	0.3428	0.3110	0.3034
9β*-NT/SA	0.3169	0.3041	0.3017
Analytical		0.3024	

Table 5.13: Scordelis-Lo roof: Center displacement u_{3_A}

Element	Unit extensional u_{1_A}	In-plane shear u_{2_A}	Out-of-plane shear u_{3_A}	Twisting forces ψ_{1_A}
Regular mesh				
5β/SA	0.3000E-04	0.1073	0.4235	0.03015
QC9D/SA	0.3000E-04	0.1055	0.4235	0.03015
8β-NC/SA	0.3000E-04	0.3794	0.4235	0.03015
8β-NT/SA	0.3000E-04	0.1072	0.4235	0.03015
9β-NC/SA	0.3000E-04	0.3794	0.4235	0.03015
9β-NT/SA	0.3000E-04	0.1072	0.4235	0.03015
QC9D*/SA	0.3000E-04	0.1055	0.4235	0.03015
8β*-NC/SA	0.3025E-03	0.3794	0.4235	0.03015
8β*-NT/SA	0.3000E-04	0.1072	0.4235	0.03015
9β*-NC/SA	0.3543E-03	0.3794	0.4235	0.03015
9β*-NT/SA	0.3000E-04	0.1072	0.4235	0.03015
Parallelograms				
5β/SA	0.3000E-4	0.06858	0.4226	0.02722
QC9D/SA	0.3000E-4	0.05519	0.4226	0.02722
8β-NC/SA	0.3000E-4	0.1530	0.4226	0.02722
8β-NT/SA	0.3000E-4	0.06640	0.4226	0.02722
9β-NC/SA	0.3000E-4	0.1519	0.4226	0.02722
9β-NT/SA	0.3000E-4	0.06169	0.4226	0.02722
QC9D*/SA	0.3000E-4	0.09868	0.4226	0.02722
8β*-NC/SA	0.3000E-4	0.2838	0.4226	0.02722
8β*-NT/SA	0.3000E-4	0.1061	0.4226	0.02722
9β*-NC/SA	0.3000E-4	0.2837	0.4226	0.02722
9β*-NT/SA	0.3000E-4	0.1048	0.4226	0.02722
Trapezoidals				
5β/SA	0.3000E-4	0.005859	0.4163	0.02834
QC9D/SA	0.3000E-4	0.004612	0.4163	0.02834
8β-NC/SA	0.3000E-4	0.01685	0.4163	0.02834
8β-NT/SA	0.3000E-4	0.005226	0.4163	0.02834
9β-NC/SA	0.3000E-4	0.01685	0.4163	0.02834
9β-NT/SA	0.3000E-4	0.005022	0.4163	0.02834
QC9D*/SA	0.3000E-4	0.09494	0.4163	0.02834
8β*-NC/SA	0.3000E-4	0.2611	0.4163	0.02834
8β*-NT/SA	0.3000E-4	0.1064	0.4163	0.02834
9β*-NC/SA	0.3000E-4	0.2610	0.4163	0.02834
9β*-NT/SA	0.3000E-4	0.1063	0.4163	0.02834
Beam theory	0.3000E-4	0.1081	0.4321	0.03208

Table 5.14: Slender cantilever: Numerical results